ISSN 2040-8978

# Journal of Optics

Volume 15 Number 7 July 2013

Journal of the European Optical Society

## Review Article

**Fano resonances and topological optics: an interplay of far- and near-field interference phenomena**

*B S Luk'yanchuk, A E Miroshnichenko and Yu S Kivshar*

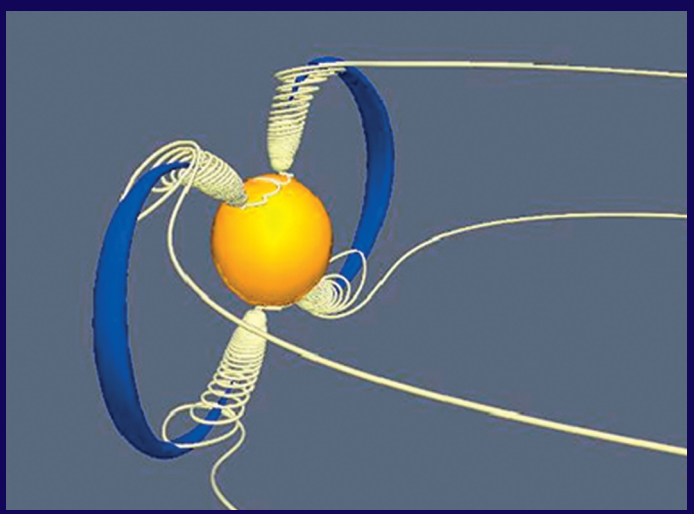

iopscience.org/jopt

IOP Publishing EOS

IOP Publishing Journal of Optics
J. Opt. **15** (2013) 073001 (8pp) doi:10.1088/2040-8978/15/7/073001

REVIEW ARTICLE

# Fano resonances and topological optics: an interplay of far- and near-field interference phenomena*

**B S Luk'yanchuk**[1], **A E Miroshnichenko**[2] **and Yu S Kivshar**[2]

[1] Data Storage Institute, Agency for Science, Technology and Research, 117608, Singapore
[2] Nonlinear Physics Centre, Research School of Physics and Engineering Australian National University, Canberra ACT 0200, Australia

E-mail: aem124@physics.anu.edu.au

Received 21 February 2013, accepted for publication 10 April 2013
Published 3 May 2013
Online at stacks.iop.org/JOpt/15/073001

**Abstract**
Fano resonances and optical vortices originate from two types of interference phenomena. Usually, these effects are considered to be completely independent, and in many cases Fano resonances are observed without any link to vortices, as well as vortices with a singular phase structure that are not accompanied by Fano resonances. However, this situation changes dramatically when we study light scattering at the nanoscale. In this paper, we demonstrate that Fano resonances observed for light scattering by nanoparticles are accompanied by the singular phase effects usually associated with singular optics, and we introduce and describe optical vortices with characteristic core sizes well below the diffraction limit.

**Keywords:** singular optics, Fano resonance, optical vortices, Mie scattering

(Some figures may appear in colour only in the online journal)

## 1. Introduction

The fascinating physics of optical wave interference offers two classes of important phenomena: optical vortices and Fano resonances. Optical vortices are observed in the structure of the wave phase that carries topological singularities or dislocations of the wavefront, which are associated with so-called *singular optics*. Fano resonances are associated with a sharp asymmetric variation of the wave transmission [1, 2]. In general, these two phenomena seem completely unrelated, such that Fano resonances are observed without topological effects as well as singular optics that is not accompanied by Fano resonance effects. However, the situation changes dramatically as soon as we reduce the size of the scattering structure and approach the nanoscale. In particular, such effects can be found for weakly dissipative metallic nanoparticles. Important peculiarities of the far-field scattering and near-field Poynting vector flux are manifested in the so-called 'nano-Fano resonances' introduced and discussed below. Control of the orbital angular momentum of photons with the help of nanostructures is a novel research direction which is very attractive for many applications in quantum optics and information technology, opening an innovative way to manipulate optical vortices at the nanoscale that may lead to new applications in near-field holography, ultra-dense optical recording, subwavelength whispering gallery modes and periodic structures.

To demonstrate our basic idea, we consider the simplest problem of light scattering by a spherical particle. For our analysis, we employ the analytical Mie theory, which allows us to get a deeper insight into the relation between the near-field and far-field interference phenomena associated with topological optics and Fano resonances, respectively. The fascinating phenomenon of Fano resonances refers to the

* This paper was an intended contribution to the special issue on singular optics (iopscience.iop.org/2040-8986/page/Special%20issue%20on%20singular%20optics).

 

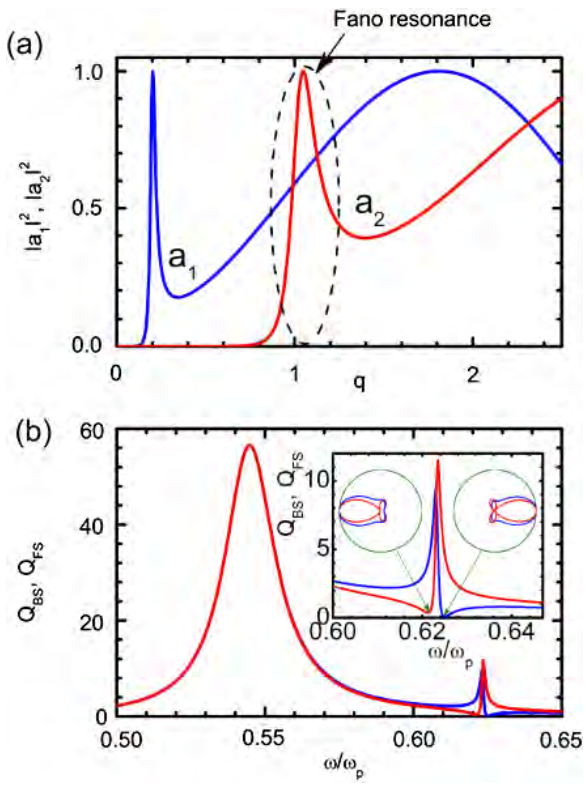


**Figure 1.** (a) Dipole $|a_1|^2$ (blue) and quadrupole $|a_2|^2$ (red) electrical scattering amplitudes versus the size parameter $q$ at $\varepsilon \approx -2.1$. (b) Backward scattering (BS; red) and forward scattering (FS; blue) cross-sections versus normalized frequency $\omega/\omega_p$. The dielectric permittivity $\varepsilon$ is described by the Drude formula, $\gamma/\omega_p = 10^{-3}$ (weak dissipation), where $\omega_p$ is the plasma frequency and $\gamma$ is the collision frequency. Parameter $q = \omega_p R/c = 0.7$. Inset shows polar scattering diagrams in the $x$–$z$ plane (azimuthal angle $\varphi = 0$ in the Mie theory) near the quadrupole resonance of a plasmonic particle. The red curve corresponds to linearly polarized light; blue lines represent non-polarized light.

interference between broad and narrow spectral radiation [1, 2]. In the vicinity of a narrow spectral line, there is a $\pi$-phase jump, leading to constructive and destructive interference phenomena with a broad spectral line. Such a coexistence of constructive and destructive interference results in the characteristic asymmetric Fano lineshape. In the case of light scattering by small plasmonic particles, the dipole Rayleigh scattering plays the role of the broad spectral radiation, while the surface plasmon resonance (e.g. quadrupole or higher order resonance) plays the role of a narrow spectral line interacting with the broad spectral radiation. In the framework of the well-known Mie theory [3, 4], such a Fano resonance can be observed in the differential scattering efficiency cross-sections. In terms of the interference of electrical or magnetic scattering amplitudes (namely, $a_\ell$ or $b_\ell$ defined within the Mie theory [3, 4]), it resembles an overlap of broad and narrow spectral lines, for example, broad dipole and narrow quadrupole lines (see figure 1). Within the Mie theory, the scattering amplitudes are defined by the well-known formulas:

$$a_\ell = \frac{\Re_\ell^{(a)}}{\Re_\ell^{(a)} + \mathrm{i}\,\Im_\ell^{(a)}}, \qquad b_\ell = \frac{\Re_\ell^{(b)}}{\Re_\ell^{(b)} + \mathrm{i}\,\Im_\ell^{(b)}}, \tag{1}$$

where the functions $\Re$ and $\Im$ are combinations of the spherical Bessel and Neumann functions, see details in [4]. The resonances correspond to the condition $\Im_\ell^{(a,b)} = 0$, and for nondissipative materials these conditions correspond to the conditions $a_\ell, b_\ell = 1$.

Figure 1(a) shows the dependence of the scattering amplitudes on the Fano size parameter $q$. These dependences display two distinct peaks associated with the resonances at $q = 0.2$ (for the dipole mode) and $q = 1$ (for the quadrupole mode). For nondissipative materials, these resonances correspond to the conditions $a_\ell = 1$. Periodically repeated 'broad' maxima in the case of dielectric particles correspond to volume dipole resonances. We notice, here, that in the case of metallic particles these maxima do not correspond to resonant excitation of plasmons. Usually, for small particles the dipole scattering is dominant, $|a_1| \gg |a_2|$. Comparable amplitudes $|a_1|$ and $|a_2|$ arise when the size parameter $q$ become of the order of unity (see figure 1(a)). At the same time, for the Fano resonance we need these two amplitudes to be comparable. Thus, with a small size parameter $q$ one of the scattering amplitudes is with necessity very small. As a result, the Fano resonance is 'not pronounced' for $q \ll 1$. However, two scattering modes can interfere either constructively or destructively.

However, it is possible to generate Fano resonances within nanostructures with a very small size parameter $q \ll 1$ associated with very weak scattering. The fascinating property of such structures is related to the coexistence of the Fano resonance and topological optics effects, where the characteristic size of vortices is well beyond the diffraction limit. This property can be found, for example, in weakly dissipative plasmonic nanoparticles in the framework of the Mie theory (see figure 2). Below, we demonstrate that the limitation $q \approx 1$ for pronounced Fano resonances can be overcome for cylindrical plasmonic structures, which exhibit a Fano resonance at the nanoscale, $q \ll 1$.

## 2. Scaling of the Fano resonance for spherical nanoparticles

The basic problem with scaling of the Fano resonance can be observed for nondissipative plasmonic nanoparticles within the framework of the Mie theory. As mentioned above, the problem of Mie scattering can be solved analytically for a metallic sphere, where we can employ the exact Mie solutions [3, 4]. We find the Fano resonance in the analysis of the directional scattering efficiencies for the forward (FS) and backward scattering (BS). These scattering efficiencies are given by [1]

$$Q_{\mathrm{BS}} = \frac{1}{q^2}\left|\sum_{\ell=1}^{\infty}(2\ell+1)\,(-1)^\ell\,[a_\ell - b_\ell]\right|^2, \qquad Q_{\mathrm{FS}} = \frac{1}{q^2}\left|\sum_{\ell=1}^{\infty}(2\ell+1)\,[a_\ell + b_\ell]\right|^2. \tag{2}$$

For $q \ll 1$ one can expand the scattering amplitudes with accuracy to the $q^5$ terms as follows

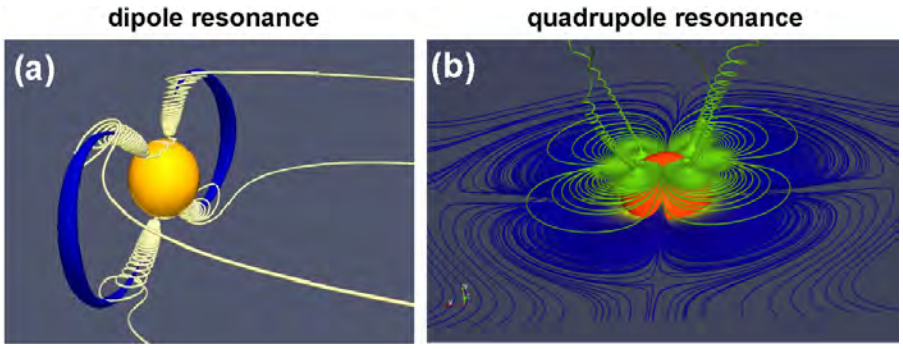


**Figure 2.** 3D Poynting vector plot for a spherical particle with the size parameter $q = 0.3$ for (a) dipole and (b) quadrupole resonances with $\varepsilon = -2.222\,8525$ and $\varepsilon = -1.533\,484$, respectively. Blue segments in panel (a) represent the surface $|S| < 0.01$, and yellow lines indicate typical Poynting vector lines encircling singularities.

$$a_1 = -\frac{2\mathrm{i}}{3}\frac{\varepsilon-1}{\varepsilon+2}q^3 - \frac{2\mathrm{i}}{5}\frac{(\varepsilon-1)(\varepsilon-2)}{(\varepsilon+2)^2}q^5, \qquad a_2 = -\frac{\mathrm{i}}{15}\frac{\varepsilon-1}{2\varepsilon+3}q^5, \tag{3}$$

$$b_1 = -\frac{\mathrm{i}}{45}q^5(\varepsilon-1), \qquad b_2 = 0. \tag{4}$$

Importantly, the expansions contain singularities in the electric amplitudes, e.g. in the dipole amplitude $a_1$ at $\varepsilon = -2$ (this singularity is seen in the formula for the Rayleigh scattering), in the quadrupole amplitude $a_2$ at $\varepsilon = -3/2$, etc. Note that the magnetic amplitudes $b_\ell$ do not have singularities.

However, there are no real singularities at exact plasmon resonances where $\Im_\ell^{(a)} = 0$. The electrical field amplitudes $a_\ell$ tend to unity at the corresponding resonant frequencies, as can be seen clearly from equation (1). This means that the Rayleigh approximation is not applicable at the points of plasmon resonances where the Rayleigh scattering is replaced by anomalous light scattering [5, 6]. To escape singularities of the scattering amplitudes, it is sufficient to expand the numerator and denominator in equation (1) independently. However, it is not so important for the determination of the anisotropy in scattering, where the positions of the forward scattering and backward scattering resonances can be found from equations (3) and (4) with sufficient accuracy. Applying the expansions (3) and (4) to equations (2) one finds that the solution of the equations $Q_{\mathrm{FS}} = 0$ and $Q_{\mathrm{BS}} = 0$ yields the size parameters

$$q^2 = q_{\mathrm{FS}}^2 = 15\,\frac{(\varepsilon+2)(2\varepsilon+3)}{(1-\varepsilon)\left(38+27\varepsilon+\varepsilon^2\right)}, \qquad q^2 = q_{\mathrm{BS}}^2 = 15\,\frac{(\varepsilon+2)(2\varepsilon+3)}{70+29\varepsilon-10\varepsilon^2+\varepsilon^3}. \tag{5}$$

Both quantities $q_{\mathrm{FS}}(\varepsilon)$ and $q_{\mathrm{BS}}(\varepsilon)$ vanish in the vicinity of the dipole ($\varepsilon \to -2$) and quadrupole ($\varepsilon \to -1.5$) resonances, see figure 3. In figure 3, we do not show nonphysical branches of equations (5) corresponding to negative values of $q^2$.

At the corresponding frequencies, we observe the transformation of the far-field scattering diagrams typical for the Fano resonance [1, 2]. These polar diagrams are calculated in a standard way, see [4]. The corresponding scattering intensities are

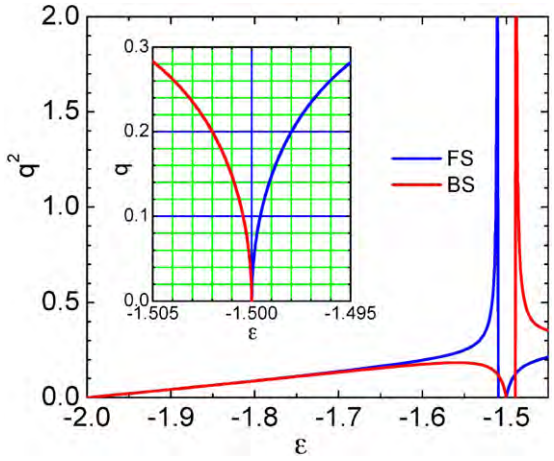


**Figure 3.** Scattering efficiencies versus permittivity. The forward scattering efficiency vanishes along the blue curve given by the first equation (5). Red curve corresponds to the second equation (5) and presents the backscattering efficiency. Inset is the region of small $q$.

$$I_{\mathrm{II}}^{(\mathrm{s})} = C\left|\sum_{\ell=1}^{\infty}(-1)^\ell\left[{}^eB_\ell P_\ell^{(1)\prime}(\cos\theta)\sin\theta - {}^mB_\ell\frac{P_\ell^{(1)}(\cos\theta)}{\sin\theta}\right]\right|^2,$$
$$I_{\perp}^{(\mathrm{s})} = C\left|\sum_{\ell=1}^{\infty}(-1)^\ell\left[{}^eB_\ell\frac{P_\ell^{(1)}(\cos\theta)}{\sin\theta} - {}^mB_\ell P_\ell^{(1)\prime}(\cos\theta)\sin\theta\right]\right|^2. \tag{6}$$

Here $C$ is the normalization coefficient; other values are the same as in [4]. For small values of the size parameter $q \ll 1$ one can see the Fano resonance in weakly dissipated plasmonic nanoparticles. The asymmetrical shapes in differential scattering efficiencies are shown in figure 4 in the vicinity of the quadrupole resonance. The variation of the scattering diagrams from forward scattering to backward scattering is shown in the circular insets to figure 4.

## 3. Formation of vortices within the Mie theory

Another type of interference phenomena is related to singular optics and the formation of vortices and dislocations of the

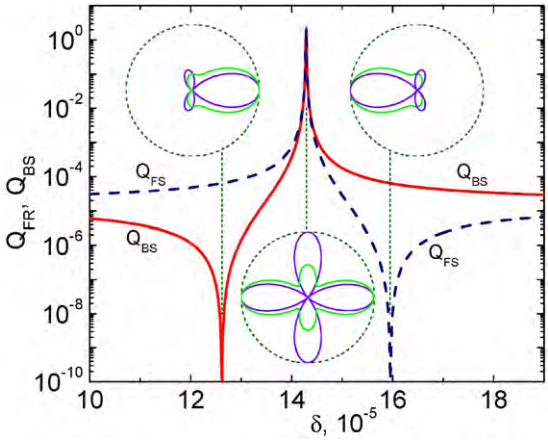


**Figure 4.** Scattering efficiencies $Q_{FS}$ and $Q_{BS}$ for the particle with $q = 0.02$ versus $\varepsilon$. Insets show the far-field scattering diagrams at the corresponding frequencies, calculated with equations (6) at the corresponding frequencies: $\varepsilon_1 = -1.5 - \delta_1$, where $\delta_1 = 1.67 \times 10^{-5}$ corresponds to zero forward scattering, $\varepsilon_2 = -1.5 + \delta_2$, where $\delta_2 = 1.67 \times 10^{-5}$ corresponds to zero backward scattering.

wavefront [7–11]. The basic point of the topological optics is the undefined phase of the electromagnetic field at points where the intensity of the wave is zero. Any $2\pi n$ phase values can be continuously conjugated at this point. The integer $n$ represents the so-called topological charge, which shows the number of twists of the phase front. There are many methods to create optical vortices by diffraction, computer generated holograms and spatial light modulators. Recently, it was shown that vortices can be created through light scattering by plasmonic nanostructures [11–13]. For weakly dissipating plasmonic spheres, vortices can be seen in the vicinity of dipole and quadrupole plasmon resonances, see the examples in [12–14].

Distribution of the Poynting vector for nondissipative plasmonic material and a small size parameter $q = 0.02$ at the points that correspond to symmetrical quadrupole resonance and forward and backward scattering are presented in figure 5. One can see large modifications of the vortex structures in the near field. Note, here, that these vortices are created during light scattering of the plane wave, in contrast to [15], where a special emitter of whispering gallery modes was used.

The lowest order Fano resonance within plasmonic nanoparticles arises due to interference of an electric dipole and an electric quadrupole [1]. Pronounced interference occurs when both interfering amplitudes are comparable at the same frequency. As we have mentioned above, this occurs when the size parameter $q$ is of the order of unity. With small size parameter, $q \to 0$, these dipole and quadrupole resonances arise at different frequencies, corresponding to $\varepsilon = -2$ for the dipole and $\varepsilon = -1.5$ for the quadrupole. Thus the interference occurs in the range of frequencies where one of the interference amplitudes is small. For example when $q = 0.1$ the dipole amplitude is five orders of magnitude smaller than the quadrupole amplitude in the range of interference. Thus it is very questionable whether one would see a Fano resonance during light scattering by a small sphere. Unfortunately a similar effect takes place on the hybridization

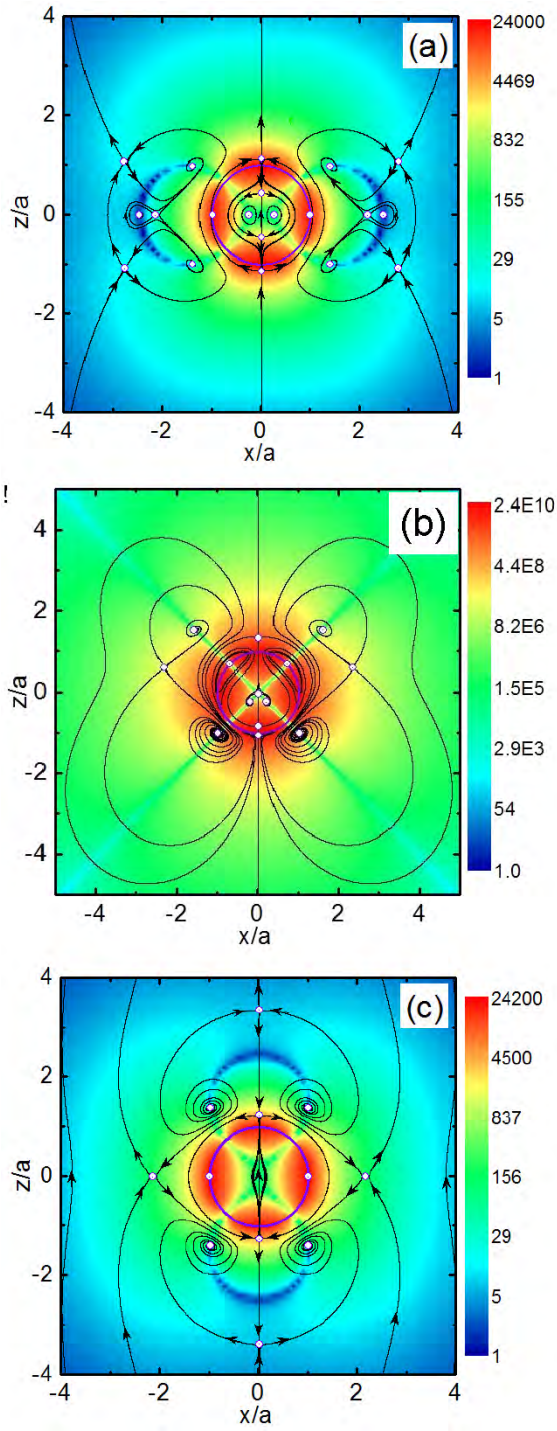


**Figure 5.** Poynting vector field in the vicinity of the quadrupole resonance at $q = 0.02$. Panels (a)–(c) correspond to different values of $\varepsilon$ with the far-field scattering diagrams shown in figure 4.

diagrams for the majority of plasmonic nanostructures, i.e. the dipole and quadrupole resonances require different values of $\varepsilon$ as $q \to 0$. This reveals that the Fano resonance is in fact forbidden in nanostructures with a size much smaller than the wavelength.

The distributions of the Poynting vector for nondissipative plasmonic nanoparticles and small $q = 0.02$ at the points corresponding to symmetrical quadrupole resonance

and forward and backward scattering are shown in figure 5. We observe modifications of the vortex structures in the near field.

## 4. Scaling Fano resonances in plasmonic nanostructures

Although a majority of plasmonic structures with Fano resonances suffer from scaling, there exists an important conformance exception for structures with cylindrical symmetry. For such structures all surface plasmon resonances at small size parameter $q \to 0$ start from the same value $\varepsilon = -1$. This, in principle, permits the creation of Fano resonances with extreme nano-sizes in the visible regime, see figure 6. Here $\bar{a}_i$ denotes the corresponding amplitude of electric scattering coefficients within the Mie theory for a cylinder [16–18]. Here, a bar is used to distinguish scattering amplitudes for spheres and cylinders. The surface plasmons in the cylindrical nanowire are excited in the case of perpendicular polarization $\mathbf{E} \perp z$ (TE-mode) and are not excited with $\mathbf{E} \parallel z$ (TM-mode) [16]. For the case of the TE-mode and normal incidence, the scattering efficiency $Q_{\text{sca}}$ is expressed by

$$Q_{\text{sca}} = \frac{2}{q} \sum_{\ell=-\infty}^{\infty} |\bar{a}_\ell|^2. \tag{7}$$

In this definition of $q = kR$, $R$ is the physical radius of the nanowire. The scattering amplitudes $\bar{a}_\ell$ (electric) are defined by the well-known formulas [3, 16]. However, it is convenient to write these formulas by separating the real and imaginary parts

$$\bar{a}_\ell = \frac{\Re_\ell}{\Re_\ell + \mathrm{i}\,\Im_\ell}. \tag{8}$$

Functions $\Re_\ell$ and $\Im_\ell$ are given by:

$$\begin{aligned} \Re_\ell &= nJ_\ell(nq)J'_\ell(q) - J'_\ell(nq)J_\ell(q), \\ \Im_\ell &= nJ_\ell(nq)N'_\ell(q) - J'_\ell(nq)N_\ell(q), \end{aligned} \tag{9}$$

where $J_\ell(z)$ and $N_\ell(z)$ are the Bessel and the Neumann functions. The primes in (11) indicate differentiation with respect to the argument of the function, i.e. $J'_\ell(z) \equiv \mathrm{d}J_\ell(z)/\mathrm{d}z$, etc. The refractive index $n = \sqrt{\varepsilon}$, where $\varepsilon$ is the relative dielectric permittivity $\varepsilon = \varepsilon_{\text{p}}/\varepsilon_{\text{m}}$. Indices 'p' and 'm' indicate wire and ambient media, respectively. The coefficients $a_\ell$ are symmetrical: $\bar{a}_{-\ell} = \bar{a}_\ell$. The scattering cross-section is defined as $\sigma_{\text{sca}} = 2RLQ_{\text{sca}}$, where $2RL$ is a geometrical cross-section (the length of the cylinder $L \gg R$). In the case of nondissipative material, $\mathrm{Im}\varepsilon = 0$, amplitudes $\bar{a}_\ell$ reach maximal value $\bar{a}_\ell = 1$ along the trajectories on the $\{\varepsilon, q\}$ plane given by the equation $\Im_\ell(\varepsilon, q) = 0$. Three trajectories for $\ell = 1$ (dipole), $\ell = 2$ (quadrupole) and $\ell = 3$ (octopole) are shown in figure 6.

The lowest Fano resonance appears due to the interference of dipole and quadrupole modes. Similar to its spherical counterpart [1], this resonance can be predicted and interpreted with differential forward and back scattering

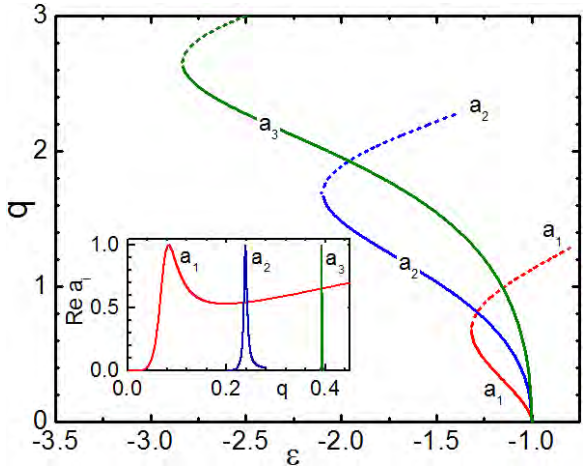


**Figure 6.** Trajectories of the first three optical electric resonances: $a_1$ (dipole), $a_2$ (quadrupole) and $a_3$ (octopole) for a cylinder. Insets show plots of dipole (red), quadrupole (blue) and octopole (green) resonances versus the size parameter at $\varepsilon = -1.02$. The monopole mode $a_0$ for a cylinder is not shown because it is situated at high $q$ values, see [16].

cross-sections, $Q_{\text{FS}}$ and $Q_{\text{BS}}$. These cross-sections for cylinders can be defined by the formulas:

$$Q_{\text{FS}} = \frac{2}{\pi q}|f_0|^2, \qquad Q_{\text{BS}} = \frac{2}{\pi q}|f_\pi|^2, \tag{10}$$

where

$$\begin{aligned} f_0 &= \sum_{\ell=-\infty}^{\infty} (-\mathrm{i})^\ell \mathrm{e}^{-\mathrm{i}\pi\ell/2}\bar{a}_\ell, \\ f_\pi &= \sum_{\ell=-\infty}^{\infty} (-\mathrm{i})^\ell (-1)^\ell \mathrm{e}^{-\mathrm{i}\pi\ell/2}\bar{a}_\ell. \end{aligned} \tag{11}$$

When the size parameter is of the order of unity, we observe the Fano resonance related to an overlap of different modes, e.g., dipole–quadrupole and dipole–octopole interference, similar to Mie theory for spheres. However, with $q \ll 1$ in cylindrical structures all surface plasmon resonances converge at $\varepsilon = -1$. This permits the existence of a nanoscale Fano resonance in visible light. Hence, we find that the Fano resonance has no size limitation in the cylindrical configuration with nondissipative media.

An attractive property of plasmonic structures with a Fano resonance is that the spatial distribution of scattered light depends strongly on the frequency [16]. In the vicinity of the Fano resonance, the far-field radiation exhibits strong asymmetry in the radiation pattern, as depicted in figure 7. In figure 8, we show the scattering diagrams for frequencies near the Fano resonance for a nondissipative plasmonic cylinder. The switching is very sensitive to the perturbation of the frequency of the incident light (consequently a perturbation in material permittivity), which is verified in figure 8. It is important that this variation with cylindrical structures can be reached with a very small size parameter $q \ll 1$. It can be employed in such applications as optical storage, sensing or optical switching.

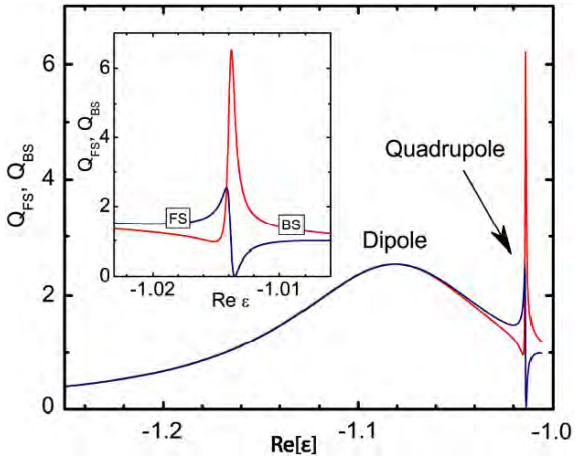


**Figure 7.** Forward and backward scattering cross-sections for a nanowire with size parameter $q = 0.2$. The inset is a zoomed-in view near the new Fano resonance for nanoparticles.

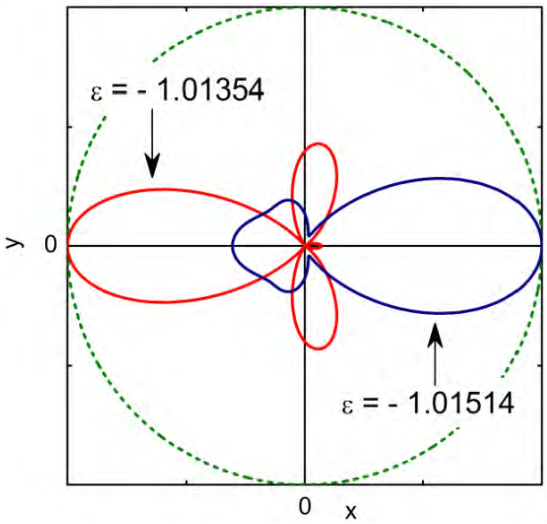


**Figure 8.** The scattering diagrams for frequencies near the Fano resonance for a cylinder with a size parameter $q = 0.2$. A dramatic variation in scattering arises with $\Delta\varepsilon/\varepsilon \approx 1.6 \times 10^{-3}$.

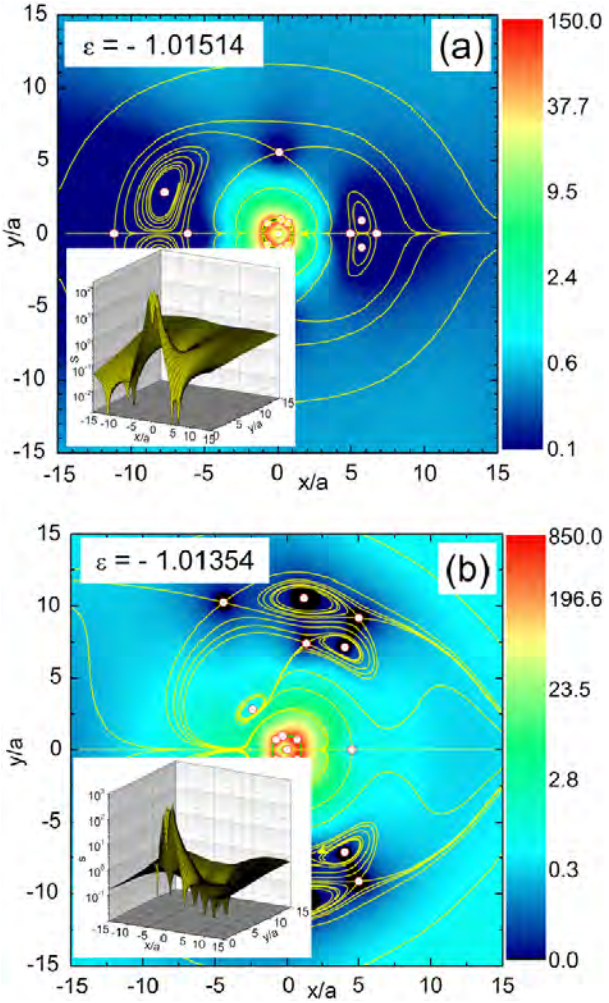


**Figure 9.** Poynting vector field for light scattering by a nondissipative plasmonic cylinder with a size parameter $q = 0.2$. The two pictures correspond to the forward and backward scattering diagram in figure 7. The background color in the contour plot indicates the absolute value of the Poynting vector $S = \sqrt{S_r^2 + S_\varphi^2}$ (logarithmic scale, see 3D plots in the insets). The lines show separatrices of the Poynting vector. Red circles indicate the singular points. In the case of forward scattering (a) one can see 14 singular points out of the particle and four optical vortices; in (b) there are 14 singular points and six optical vortices. The insets show the magnitude of the energy flux $S$ in the $x$–$y$ plane.

## 5. Vortices near the Fano resonance in plasmonic nanowires

Light scattering by a thin nanowire with a surface plasmon resonance is accompanied by bifurcations of the Poynting vector field exhibiting singular points and optical vortices [16]. In contrast to the vortices shown in figure 5, optical vortices in cylindrical structures appear near the well-pronounced Fano resonance, similar to that shown in figure 7. An example of vortices in the near-field scattering of cylindrical structures with a Fano resonance can be seen in the distributions of the Poynting vector shown in figure 9.

A majority of practically realized optical vortices have characteristic scales greater than the diffraction limit, e.g. the core of an optical vortex is of the order of 10 $\mu$m [15]. In contrast, here we demonstrate optical vortices localized on a scale smaller than 100 nm, i.e. two orders of magnitude smaller. Thus, these 'nano-Fano' resonances provide a route towards nanoscale optical vortices substantially different from conventional optical beams. The unique ability to control the topology of the electromagnetic wave distribution by small variations of the light frequency in the vicinity of the Fano resonance looks very promising for applications of topological optics, e.g. in quantum optics.

## 6. Near-field topology of dielectric nanoparticles

Recently, dielectric nanoparticles have attracted much attention due to their ability to support magnetic dipole resonances in the visible range [19–21]. Moreover, in contrast to their plasmonic counterparts, dielectric particles can simultaneously support electric and magnetic modes of the

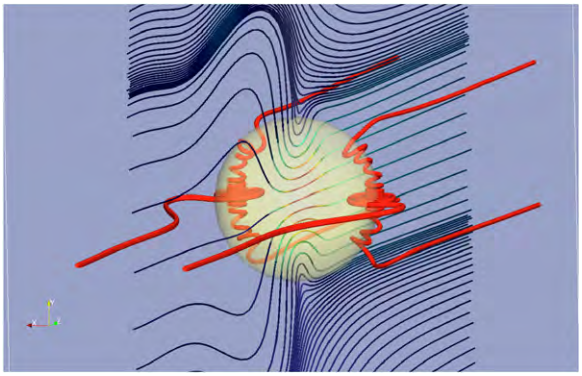

**Figure 10.** Poynting vector energy flow for a dielectric particle at the magnetic resonance for a size parameter $q = 1$ and $\varepsilon = 9.1$. Red lines show characteristic separatrices.

same strength. This opens up new and unique possibilities for interference phenomena. In particular, it was experimentally demonstrated that a single dielectric nanoparticle acts as an efficient optical antenna with a relatively high directivity and a large front-to-back ratio due to constructive interference of electric and magnetic dipole modes in the forward scattering direction [22, 23]. This effect is directly associated with the directional Fano resonance, where the magnetic dipole mode is at the resonance and the electric dipole mode plays the role of the broad nonresonant background. This kind of response can be further enhanced by arranging such particles in an appropriate configuration, e.g. in a finite array of optical nanoantennas [24–27] or oligomer-like structures [28]. Another interesting effect is the capability for 3D subwavelength light confinement outside a dielectric sphere, known as a photonic nanojet [29–32]. It is believed to be associated with the formation of vortices in the near field, but more studies are required to investigate the phenomenon in detail.

In figure 10 we plot the Poynting vector power flow of a dielectric particle at the magnetic resonance. Although it looks similar to the power flow for the electric dipole resonance of the plasmonic nanoparticle, there are a couple of differences. The energy flow is maximal inside the dielectric nanoparticle, increasing towards the center. Due to the positive index of refraction there is no discontinuity of the energy flow at the nanoparticle boundary. There is no clear singularity, but still there is strong energy flow around the spherical particle along the surface, leading to the enhancement of the power flow through the nanoparticle. This is still a preliminary result, and it deserves further investigation.

## 7. Concluding remarks

Scaling of the Fano resonances in nanostructures has been discussed in a few papers, see e.g. [2, 5, 18, 33]. Typically, a pronounced Fano resonance can be observed for structures with a size parameter of the order of unity. In practice, the smallest experimentally realized plasmonic structures demonstrating Fano resonances have characteristic sizes of 100 nm and above [5]. A challenge with Fano resonance scaling is that it has a deep physical underpinning related to the different resonance frequencies of the interfering resonances, which lead to strong suppression of the Fano resonance for nanostructures with small values of the size parameter.

Here, we have studied the scaling of the Fano resonance for nanostructures with both spherical and cylindrical symmetries. We have found that the cylindrical geometry is less sensitive to the material dissipation than the spherical geometry. In contrast to spherical nanostructures, all surface plasmon resonances in small cylindrical metallic structures appear at the same frequency, corresponding to the value $\varepsilon = -1$. This permits scaling and allows one to find an intricate interconnection between the near-field distribution and the far-field scattering. The attractive property of small plasmonic structures is the coexistence of the Fano resonance and singular optics effects, which allows one to control optical vortices at the nanoscale, with the size of the vortices being two orders of magnitude smaller than the conventional vortices discussed previously [9, 34].

As we mentioned above, the realization of such 'nano-Fano' structures requires materials with weak dissipation. In addition to natural low loss materials such as K, Na and Al, a promising way is to synthesize new weakly dissipative materials such as alloys [35]. Another approach is to compensate the losses by employing the concept of active plasmonics [36] or to use anisotropy effects [37, 36]. The realization of extremely small structures with a pronounced Fano resonance is very attractive for data storage technology, nanosensors, and topological optics. A more detailed analysis of the singular optics effects will be published in a chapter of a forthcoming book [38].

## Acknowledgments

We thank Drs Z B Wang, A I Kuznetsov, D L Gao, C-W Qiu, G Vienne, R Bakker and A Desyatnikov for useful discussions. This work was supported by the Agency for Science, Technology and Research (A*STAR) of Singapore: SERC Metamaterials Program on Superlens, grant no. 092 154 0099; SERC grant no. TSRP-1021520018; grant no. JCOAG03-FG04-2009 from the Joint Council of A*STAR. The work of AEM and YSK was supported by the Australian Research Council.

## References

[1] Luk'yanchuk B, Zheludev N I, Maier S A, Halas N J, Nordlander P, Giessen H and Chong T C 2010 The Fano resonance in plasmonic nanostructures and metamaterials *Nature Mater.* **9** 707
[2] Miroshnichenko A E, Flach S and Kivshar Yu S 2010 Fano resonances in nanoscale structures *Rev. Mod. Phys.* **82** 2257
[3] Bohren C F and Huffman D R 1998 *Absorption and Scattering of Light by Small Particles* (New York: Wiley)
[4] Born M and Wolf E 1999 *Principles of Optics* 7th edn (Cambridge: Cambridge University Press)
[5] Tribelsky M I and Luk'yanchuk B S 2006 Anomalous light scattering by small particles *Phys. Rev. Lett.* **97** 263902

[6] Luk'yanchuk B, Miroshnichenko A E, Tribelsky M I, Kivshar Y S and Khokhlov A R 2012 Paradoxes in laser heating of plasmonic nanoparticles *New J. Phys.* **14** 093022

[7] Nye J F and Berry M V 1974 Dislocations in wave trains *Proc. R. Soc.* A **336** 165

[8] Soskin M S and Vasnetsov M V 2001 Singular optics *Prog. Opt.* **42** 219

[9] Dennis M R, O'Holleran K and Padgett M J 2009 Singular optics: optical vortices and polarization singularities *Prog. Opt.* **53** 293

[10] Desyatnikov A S, Kivshar Y S and Torner L 2005 Optical vortices and vortex solitons *Prog. Opt.* **47** 291–391

[11] Yi X, Miroshnichenko A E and Desyatnikov A S 2012 Optical vortices at Fano resonances *Opt. Lett.* **37** 4985

[12] Wang Z B, Luk'yanchuk B S, Hong M H, Lin Y and Chong T C 2004 Energy flows around a small particle investigated by classical Mie theory *Phys. Rev.* B **70** 035418

[13] Bashevoy M V, Fedotov V A and Zheludev N I 2005 Optical whirlpool on an absorbing metallic nanoparticle *Opt. Express* **13** 8372

[14] Luk'yanchuk B S, Wang Z B, Tribelsky M, Ternovsky V, Hong M H and Chong T C 2007 Peculiarities of light scattering by nanoparticles and nanowires near plasmon resonance frequencies *J. Phys.: Conf. Ser.* **59** 234

[15] Cai X, Wang J, Strain M J, Johnson-Morris B, Zhu J B, Sorel M, O'Brien J L, Thompson M G and Yu S 2012 Integrated compact optical vortex beam emitters *Science* **338** 363

[16] Luk'yanchuk B S and Ternovsky V 2006 Light scattering by thin wire with surface plasmon resonance: bifurcations of the Poynting vector field *Phys. Rev.* B **73** 235432

[17] Luk'yanchuk B S, Tribelsky M I, Ternovsky V, Wang Z B, Hong M H, Shi L P and Chong T C 2007 Peculiarities of light scattering by nanoparticles and nanowires near plasmon resonance frequencies in weakly dissipating materials *J. Opt. A: Pure Appl. Opt.* **9** S294

[18] Qiu C W, Novitsky A, Gao L, Dong J W and Luk'yanchuk B 2012 Anisotropy-induced Fano resonance arXiv:1202.5613v1 [physics.optics], 25 February

[19] Evlyukhin A B, Reinhardt C, Seidel A, Luk'yanchuk B S and Chichkov B N 2010 Optical response features of Si-nanoparticle arrays *Phys. Rev.* B **201** 045404

[20] Kuznetsov A I, Miroshnichenko A E, Fu Y H, Zhang J B and Luk'yanchuk B 2012 Magnetic light *Sci. Rep.* **2** 492

[21] Evlyukhin A B, Novikov S M, Zywietz U, Eriksen R L, Reinhardt C, Bozhevolnyi S I and Chichkov B N 2012 Demonstration of magnetic dipole resonances of dielectric nanospheres in the visible region *Nano Lett.* **12** 3749–55

[22] Geffrin J M *et al* 2012 Magnetic and electric coherence in forward-and back-scattered electromagnetic waves by a single dielectric subwavelength sphere *Nature Commun.* **3** 1171

[23] Fu Y H, Kuznetsov A I, Miroshnichenko A E, Yu Y and Luk'yanchuk B 2013 Directional visible light scattering by silicon nanoparticles *Nature Commun.* **4** 1527

[24] Krasnok A E, Miroshnichenko A E, Belov P A and Kivshar Y S 2011 Huygens optical elements and Yagi–Uda nanoantennas based on dielectric nanoparticles *JETP Lett.* **94** 593–8

[25] Krasnok A E, Miroshnichenko A E, Belov P A and Kivshar Y S 2012 All-dielectric optical nanoantennas *Opt. Express* **20** 20599–604

[26] Liu W, Miroshnichenko A E, Neshev D N and Kivshar Y S 2012 Broadband unidirectional scattering by magneto-electric core–shell nanoparticles *ACS Nano* **6** 5489–97

[27] Filonov D S, Krasnok A E, Slobozhanyuk A P, Kapitanova P V, Nenasheva E A, Kivshar Y S and Belov P A 2012 Experimental verification of the concept of all-dielectric nanoantennas. *Appl. Phys. Lett.* **100** 201113

[28] Miroshnichenko A E and Kivshar Y S 2012 Fano resonance in all-dielectric oligomers *Nano Lett.* **12** 6459–63

[29] Luk'yanchuk B S, Anisimov S I and Yongfeng L 2001 Dynamics of subpicosecond laser ablation, examined by moments technique *Proc. SPIE* **4423** 141–52

[30] Chen Z, Taflove A and Backman V 2004 Photonic nanojet enhancement of backscattering of light by nanoparticles: a potential novel visible-light ultramicroscopy technique *Opt. Express* **12** 1214–20

[31] Itagi A V and Challener W A 2005 Optics of photonic nanojets *J. Opt. Soc. Am.* A **22** 2847–58

[32] Ferrand P, Wenger J, Devilez A, Pianta M, Stout B, Bonod N, Popov E and Rigneault H 2008 Direct imaging of photonic nanojets *Opt. Express* **16** 6930–40

[33] Tribelsky M I, Miroshnichenko A E and Kivshar Y S 2012 Unconventional Fano resonances in light scattering by small particles *Europhys. Lett.* **97** 44005

[34] Vasnetsov M and Staliunas K 1999 *Optical Vortices* (New York: Nova Science)

[35] Boltasseva A and Atwater H A 2011 Low-loss plasmonic metamaterials *Science* **331** 290

[36] Noginov M A *et al* 2009 Demonstration of a spaser-based nanolaser *Nature* **460** 1110

[37] Luk'yanchuk B S and Qiu C-W 2008 Field enhancement in spherical particles with weakly dissipating anisotropic materials *Appl. Phys.* A **92** 773

[38] Luk'yanchuk B S, Wang Z B, Miroshnichenko A E, Kivshar Yu S, Kuznetsov A I, Gao D L, Gao L and Qiu C-W 2013 Nano-Fano resonances and topological optics *Singular and Chiral Nanoplasmonics* ed S V Boriskina and N I Zheludev (Singapore: Pan Stanford) at press